



Biodegradability of carbon nanotube/polymer nanocomposites under aerobic mixed culture conditions



Duc C. Phan^{a,b,1}, David G. Goodwin Jr.^{c,1}, Benjamin P. Frank^c, Edward J. Bouwer^a, D. Howard Fairbrother^{c,*}

^a Department of Environmental Health and Engineering, Johns Hopkins University, Baltimore, MD 21218, United States

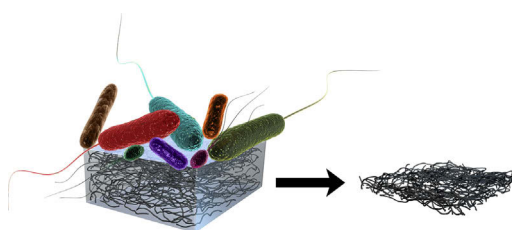
^b Department of Civil and Environmental Engineering, The University of Texas at San Antonio, San Antonio, TX 78249, United States

^c Department of Chemistry, Johns Hopkins University, Baltimore, MD 21218, United States

HIGHLIGHTS

- Polymer matrices of MWCNT/polyhydroxyalkanoate (PHA) nanocomposites were biodegraded using an aerobic mixed culture.
- The extent and rate of PHA matrix biodegradation was not affected by the presence of (0–10% w/w) MWCNTs.
- MWCNTs formed a compressed, interconnected mat with a thickness decrease of >70% after PHA biodegradation.
- The MWCNT mat formed contained the same MWCNT mass present in the initial nanocomposite, indicating a lack of MWCNT release.

GRAPHICAL ABSTRACT



ARTICLE INFO

Article history:

Received 8 March 2018

Received in revised form 9 May 2018

Accepted 11 May 2018

Available online 26 May 2018

Editor: P. Holden

Keywords:

Aerobic microbial degradation

Carbon nanotube/polymer nanocomposites

Mixed culture

Polymer nanocomposite transformation

Carbon nanotube accumulation

ABSTRACT

The properties and commercial viability of biodegradable polymers can be significantly enhanced by the incorporation of carbon nanotubes (CNTs). The environmental impact and persistence of these carbon nanotube/polymer nanocomposites (CNT/PNCs) after disposal will be strongly influenced by their microbial interactions, including their biodegradation rates. At the end of consumer use, CNT/PNCs will encounter diverse communities of microorganisms in landfills, surface waters, and wastewater treatment plants. To explore CNT/PNC biodegradation under realistic environmental conditions, the effect of multi-wall CNT (MWCNT) incorporation on the biodegradation of polyhydroxyalkanoates (PHA) was investigated using a mixed culture of microorganisms from wastewater. Relative to unfilled PHA (0% w/w), the MWCNT loading (0.5–10% w/w) had no statistically significant effect on the rate of PHA matrix biodegradation. Independent of the MWCNT loading, the extent of CNT/PNC mass remaining closely corresponded to the initial mass of CNTs in the matrix suggesting a lack of CNT release. CNT/PNC biodegradation was complete in approximately 20 days and resulted in the formation of a compressed CNT mat that retained the shape of the initial CNT/PNC. This study suggests that although CNTs have been shown to be cytotoxic towards a range of different microorganisms, this does not necessarily impact the biodegradation of the surrounding polymer matrix in mixed culture, particularly in situations where the polymer type and/or microbial population favor rapid polymer biodegradation.

© 2018 Elsevier B.V. All rights reserved.

* Corresponding author.

E-mail address: howardf@jhu.edu (D.H. Fairbrother).

¹ Both authors contributed equally to this work.

1. Introduction

Nanomaterial fillers can improve numerous polymer properties, which has led to the increasing production of polymer nanocomposites (PNCs). Tensile strength, modulus, light absorption, thermal resistance, and electrical conductivity are just a few of the properties that can be modified by the incorporation of nanomaterials into polymers (Zaman et al., 2014; Kumar et al., 2009). In particular, the high aspect ratio, durability, flame resistance, electrochemical properties, and mechanical strength of carbon nanotubes (CNTs) can markedly improve the properties of a polymer at a relatively low loading, typically between 0.1 and 5% w/w (Moniruzzaman & Winey, 2006; Sahoo et al., 2010; Du et al., 2007; Harrison & Atala, 2007; De et al., 2013). An additional benefit of CNTs is that they allow polymers to remain lightweight upon CNT incorporation as opposed to metallic additives, which can significantly increase polymer weight (De et al., 2013; Coleman et al., 2006; Sarkar et al., 2018).

The beneficial effect of CNTs on polymer properties are particularly important when the nascent properties of a polymer are improved by CNT inclusion to the extent that they become useful for certain applications (Mittal, 2011). For example, the petroleum-based polymer, poly- ϵ -caprolactone (PCL) is ideal for use in the body but requires the inclusion of CNTs to improve its mechanical strength and temporal stability in tissue scaffolding applications (Gupta et al., 2013; Pan et al., 2012; Mattioli-Belmonte et al., 2012). Another class of polymers, bio-derived polymers, often have poor physico-chemical properties including low melting points, low tensile strength, and minimal conductivity, which prevent or limit their use in a wide range of applications (Mittal, 2011; Posen et al., 2016). There is, however, considerable interest in the manufacture and use of bio-derived polymers due to low production costs, which are a result of simple synthetic routes that make use of renewable precursors derived from microorganisms, plants, and fungi (Mittal, 2011; Posen et al., 2016). For these polymers, the inclusion of CNTs can produce a dramatic improvement in their properties, facilitating their use in commercial products (Mittal, 2011). For example, <1% w/w multi-wall CNTs (MWCNTs) increases the stiffness of starch by 70% (Fama et al., 2011). Furthermore, the addition of only 0.8% w/w oxidized multi-wall CNTs (O-MWCNTs) to chitosan, a bio-derived polymer used in food packaging and filtration, improves the tensile modulus and strength by 93% and 99%, respectively (Aider, 2010; Wan Ngah et al., 2011; Miretzky & Cirelli, 2011; Wang et al., 2005).

Many of these bio-derived polymers and even some petroleum-based polymers are biodegradable. For example, PCL, poly(vinyl alcohol), poly(butylene succinate), poly(ethylene succinate), starch, cellulose, and polyhydroxyalkanoates (PHA) typically biodegrade on the order of days to months (Mittal, 2011; Tokiwa et al., 2009a; Luckachan & Pillai, 2011; Premraj & Doble, 2005). Other polymers such as chitosan and polylactides (PLA) are also biodegradable, albeit over longer time scales, and are often blended with more biodegradable polymers (Tokiwa et al., 2009a; Wu, 2005; Wu & Liao, 2007). While CNTs can enhance a range of materials properties, the inclusion of CNTs may, however, affect the biodegradation of the polymer matrix. Moreover, there is the potential for CNT exposure and release into the environment as a result of microbial degradation of PNCs post-consumer use (Mittal, 2011; Luckachan & Pillai, 2011; Stuart, 2008; Deshmukh & Mhadeshwar, 2011; Ging et al., 2014). Other types of nanomaterials, such as nanoclay and graphene oxide, have been incorporated into biodegradable polymers to assess changes in biodegradation rates. For example, nanoclay incorporation into PHB or poly(hydroxybutyrate-co-valerate) (PHB/V) led to an increased biodegradation rate of the copolymer during composting (Maiti & Prakash Yadav, 2008; Singh et al., 2011). The authors suggested that the smaller polymer spherulites formed as a result of the nanoclay incorporation increased the interfacial area available to extracellular enzymes, thereby enhancing the biodegradation rate (Maiti & Prakash Yadav, 2008;

Singh et al., 2011). In contrast to nanoclay, graphene oxide (GO) was shown to reduce polymer biodegradation due to GO cytotoxicity, but the presence of carbon-based nanofillers did not prevent the polymer from biodegrading (Peña-Bahamonde et al., 2018). CNTs are also known to be cytotoxic to a wide variety of microorganisms, (Goodwin et al., 2015; Santos et al., 2012; Lanone et al., 2013; Yang et al., 2017) and therefore have the potential to inhibit rather than accelerate biodegradation rates in the absence of structural changes to the polymer, as we have seen in our previous study using a monoculture (Goodwin et al., 2018). Several other studies have shown the accumulation of CNTs and other carbon-based nanomaterials occurs at the surface of polymer nanocomposites during aerobic mixed culture biodegradation or other environmental processes (e.g. ultraviolet weathering) (Peña-Bahamonde et al., 2018; Fan et al., 2017; Goodwin et al., 2016; Petersen et al., 2014; Nguyen et al., 2009; Kim et al., 2009). Moreover, only a select few isolated microorganisms have been shown to biodegrade CNTs and even then at extremely slow rates under optimized laboratory conditions (Parks et al., 2015; Zhang et al., 2013; Chen et al., 2017). Consequently, CNTs are expected to persist much longer in the environment than biodegradable polymers. Since their ecotoxicity is of concern, the benefits of using CNT additives during consumer use may therefore be compromised by the ultimate fate of PNCs when they enter landfills, surface waters, and/or wastewater treatment plants (De et al., 2013; Mittal, 2011; Goodwin et al., 2015; Gottschalk & Nowack, 2011; Petersen et al., 2011; Hossain et al., 2014; Freixa et al., 2018).

To date, the biodegradation behavior of CNT/PNCs containing a biodegradable polymer matrix has received little attention. In a single culture of *Pseudomonas aeruginosa*, we have previously shown that CNT fillers can impact the biodegradation kinetics and persistence of a polymer (Goodwin et al., 2018); however, it is unclear whether this behavior will persist under more environmentally relevant conditions (i.e. in the presence of an aerobic mixed culture). In one of the few studies on aerobic mixed culture biodegradation of CNT/PNCs containing biodegradable polymers, Wu et al. investigated the biodegradation of CNT/PLA nanocomposites buried in soil for five months (Wu et al., 2010). Their results showed that the presence of CNTs reduced the degradation rate, driven by both microbial and chemical processes, of PLA (Wu et al., 2010). Unlike an enzymatic study by Tsuji et al. reported that the incorporation of single-wall CNTs (SWCNTs) into PLA accelerated the enzymatic degradation of CNT/PLA nanocomposites. The authors explained that the poor interfacial interaction between the CNTs and the PLA matrix may have accelerated the degradation process by creating more PLA surface area exposed to enzymes (Tsuji et al., 2007). In contrast to the results reported by Wu and Tsuji, Zeng et al. reported that PCL grafted onto CNTs biodegraded at the same rate as pure PCL in the presence of *Pseudomonas* lipase, a bioactive enzymatic catalyst (Zeng et al., 2006).

In the present study, we have conducted a systematic investigation on the biodegradability of CNT/PNCs containing a biodegradable, bio-derived polymer (PHA) matrix exposed to an aerobic mixed culture. Primary effluent from a domestic wastewater treatment plant was used as the source of the mixed culture since it contains a wide range of microorganisms prevalent in the environment (EPA, 2001; Gilmore et al., 1993; Leja and Lewandowicz, 2010; Massardier-Nageotte et al., 2006). PHA was selected as the polymer matrix because it can be rapidly biodegraded in the environment, on the order of weeks, it is sustainably produced, (Lee et al., 1999). PHA is also being increasingly used as a substitute for traditional plastics in commercial products that include films, pins, and screws due to its low cost (Volova, 2004; Sudesh, 2012; Misra et al., 2006). Furthermore, it has been shown that CNTs can improve PHA properties for broader use in many applications (Bhatt et al., 2008; Jendrossek & Handrick, 2002; Jendrossek et al., 1993; Madbouly et al., 2014; Mas-Castellà et al., 1995; Numata et al., 2009; Ohura et al., 1999; Shah et al., 2010; Shah et al., 2008; Volova et al., 2011; Volova et al., 2010; Volova et al., 2007; Weng et al., 2011; Mergaert et al.,

1992; Armentano et al., 2010; Huh et al., 2014; Kim, 2009; Liao & Wu, 2013; Velasco-Santos et al., 2003; Yun et al., 2008). Overall, the goals of this study were to, (i) determine the effect that CNTs and CNT mass loading have on polymer biodegradation, (ii) determine the structural changes that occur to the PNC as a result of biodegradation, and (iii) assess the likelihood that CNTs will be released during the biodegradation process.

2. Experimental

2.1. CNT/PNC Preparation

Polyhydroxyalkanoates (PHA) typically consist of polyhydroxybutyrate (PHB) and polyhydroxybutyrate-hydroxyvalerate (PHB/HV), polyesters that many types of microorganisms, such as *Aeromonas hydrophila* and *Thiococcus pfennigii*, can produce and accumulate for carbon and/or energy storage (Lee et al., 1999). In this case, the PHA chosen was a co-polymer of poly-3-hydroxybutyrate (P3HB) and poly-4-hydroxybutyrate (P4HB), which was bio-derived and processed for production by Yield10Bioscience (formerly Metabolix Inc., Woburn, MA). Pristine MWCNTs at different mass loadings (% w/w) were first incorporated into PHA using solution blending methods; MWCNTs were chosen since they are the most common type of CNT blended into commercial polymer products (De et al., 2013). MWCNT/PHA nanocomposites consisting of different mass fractions of pristine multi-wall carbon nanotubes (MWCNTs, NanoLab Inc., PD15L5-20, Lot # 20130820, outer diameter 15 ± 5 nm, length $5\text{--}20$ μm) were prepared by adding the MWCNTs and a consistent mass fraction of ethylcellulose (5% w/w), hereafter abbreviated as EC (48.0–49.5% (w/w) ethoxyl basis, Lot # BCBG4792V, Sigma Aldrich), to 160 mL chloroform (CHCl_3 , HPLC grade, $\geq 99.9\%$, Sigma-Aldrich). Energy dispersive X-ray analysis (EDS) was performed on the MWCNTs used in this study to determine their residual metal content (Table S3). TGA analysis of the MWCNTs (see Fig. S4(a)) revealed that they had a low amorphous content (<3% below 300 °C). A MWCNT suspension stabilized by EC was produced by sonication using a Branson 1510 ultrasonicator bath operating at 70 watts for 3 h. During this process, the suspension was capped tightly to prevent solvent volatilization. After the MWCNT/EC suspension had been prepared, 1600 mg of polyhydroxyalkanoates were added and the mixture was sonicated for an additional 2 h to produce a casting solution. A pre-determined volume of this casting solution, discussed further in the SI, was then poured into aluminum dishes (44 mm diameter, 12.5 mm height, Fisher brand) and allowed to sit overnight under ambient conditions for solvent evaporation. The MWCNT/PHA nanocomposites generated in this way were then peeled from the aluminum dishes and consistently trimmed around the edges to have similar physical dimensions (29.4 ± 3.8 μm thickness); the MWCNT/PHA nanocomposite masses were 31.1 ± 2.1 mg. MWCNT/PHA nanocomposites were prepared with MWCNT loadings of 0.5, 1, 2, 5, and 10% w/w and all coupons contained 5% w/w EC. Neat PHA, without MWCNTs fillers, were also prepared as controls. The neat PHA and MWCNT/PHA nanocomposites prepared are shown in Fig. S1.

2.2. CNT/PNC characterization

1) Differential Scanning Calorimetry (DSC)

DSC measurements were made on all PNCs used in this study to characterize the effect of CNT loading on the degree of polymer crystallinity, a property of polymeric materials that can have an effect on biodegradation rates (Table S1) (Zhang et al., 2008; Qiu et al., 2011). DSC curves were generated using a TA instrument system operating over a temperature range of 30 °C to 180 °C with heating and cooling rates of 3 °C/min. DSC measurements were made for duplicate areas of each PNC and for at least two separately prepared coupons for each CNT loading used. The analysis of DSC curves for both the heating and cooling

processes was carried out for the first data run using TA Universal Analysis software 2000 (TA instruments, New Castle, Delaware). The enthalpy of fusion was calculated from the area of the endothermic peak using linear integration between the temperature ranges of 159 °C to 179 °C. The crystallinity was determined as the ratio of the experimental PNC enthalpy of fusion to the theoretical enthalpy of fusion (ΔH_0) for 100% crystalline PHA (146.6 J/g) (Barham et al., 1984).

2) Energy-Dispersive X-ray Analysis (EDS)

EDS was used to measure the chlorine content in PNC samples to ensure that all of the chloroform used to prepare the PNCs had evaporated during the drying process and therefore did not impact the biodegradation results. In these experiments, PHA as well as 5 and 10% (w/w) MWCNT/PHA nanocomposite samples were prepared and analyzed. For a given PNC, four 1 cm² pieces were tightly stacked and taped down to the sample stub to eliminate the iron signal from the underlying sample stub. Each PNC stack was analyzed with EDS (EDAX Genesis 4000 X-ray analysis system, detector resolution of 129 eV) in two areas.

3) Scanning Electron Microscopy (SEM)

SEM was used to analyze the surface structure and morphology of the MWCNT/PHA nanocomposites before and after biodegradation. The same approach, without any further sample preparation, was used to image the MWCNT/PHA nanocomposites at the conclusion of the biodegradation experiments. Bacterial cells were observed on these biodegraded surfaces. Samples were cut into 1 cm² pieces and sputter-coated with platinum (Quorum Technologies Polaron SC7640 Auto/Manual High Resolution Sputter Coater, 12 mA/800 V plasma current, and 5 min at 0.5 nm/min) prior to imaging with an SEM (JEOL 6700F, 10 keV, 7.0 nm working distance, LEI & SEI detectors). As-prepared PNC samples were imaged prior to biodegradation at either 10,000 \times , 15,000 \times , or 30,000 \times magnification in triplicate areas. Separately prepared PHA, 5%, and 10% w/w MWCNT/PHA nanocomposites were also imaged to assess the extent of sample-to-sample variability. The reproducibility of the data obtained on the biodegraded PNC samples was assessed by imaging two separately prepared 5% w/w MWCNT/PHA nanocomposites after 20 d of biodegradation.

Cross-sectional SEM was used to measure the change in thickness of the MWCNT/PHA nanocomposites as a result of 20 days of biodegradation. In these experiments, duplicate 5% w/w MWCNT/PHA samples and a single 10% w/w MWCNT/PHA sample were analyzed before and after 20 days of biodegradation. In these experiments, samples were trimmed into 1 cm² pieces and cryosnapped down the middle using liquid nitrogen. Cryosnapped PNCs were mounted on the side of a sample stub so that the sample cross-section plane was perpendicular to the direction of the SEM's electron beam. Sample cross-sections were imaged at 15,000 \times and thicknesses were determined in at least six areas per replicate using ImageJ software (NIH, Bethesda, MD). The thickness change was determined by subtracting the thickness of the biodegraded PNC samples from the thickness of the unexposed samples. Thickness changes may have been slightly larger than experimentally determined due to the presence of some biomass on the biodegraded nanocomposites.

4) Thermal Gravimetric Analysis (TGA)

TGA was run using an SDT Q600 instrument at 10 °C/min in the presence of argon (inert conditions) or air from 0 °C to 900 °C under inert and air conditions for the 10% w/w MWCNT/PHA nanocomposites before and after 15 d or 20 d of primary effluent exposure (both time points had similar mass loss). Air conditions were run to obtain the initial CNT content as a result of the change in the thermogram. Inert conditions were run to determine if there were any changes to the CNTs during nanocomposite biodegradation based on their thermal profile at higher temperatures (>600 °C). PHA (containing EC) was run as a

control (Fig. S3) to determine the temperature region at which PHA degradation took place in the nanocomposites. MWCNT powder was run under argon and air at 10 °C/min to characterize the amorphous carbon present, to determine the thermal stability of the MWCNTs, and to serve as a control to confirm the presence of CNTs in the initial and biodegraded MWCNT/PHA nanocomposites in the higher temperature regions of the thermal profiles (>300 °C in air and >320 °C in argon) (Fig. S4).

2.3. Aerobic biodegradation of MWCNT/PHA nanocomposites

1) Inoculum and Media Preparation

The inoculum chosen for this biodegradation study was primary treatment effluent provided by the Back River Wastewater Treatment Plant (Baltimore, MD). The inoculum was used the same day it was collected and diluted 1:10 (v/v) into basal mineral media (BMM) (see SI). A 200 mg/L sodium acetate trihydrate carbon source, which is equivalent to 35 mg/L carbon, was added as a supplemental growth substrate in the reactors. To ensure that dissolution of PHA did not occur in aqueous media, abiotic controls were also prepared using sterile BMM.

2) Setup for Aerobic Biodegradation and Abiotic Controls

To determine the biodegradation kinetics and the extent of biodegradation, the mass loss of MWCNT/PHA nanocomposites in the presence of primary effluent was measured as a function of time. Mass loss is one of several quantitative methods, such as CO₂ detection and oxygen consumption, typically used to assess aerobic biodegradation of pure polymers (Calmon et al., 2000; Itävaara & Vikman, 1996; Strotmann et al., 2004; Khatiwala et al., 2008; Pagga et al., 2001; Mohee et al., 2008; Pelegrini et al., 2016). The decision to use mass loss was motivated by its ease of use for a large set of samples, and its previous use for in situ biodegradability tests of plastic materials under an aerobic compost environment (ASTM D 6003-96) (ASTM, 1996; Krzan et al., 2006). Individual MWCNT/PHA nanocomposites with CNT loadings of 0, 0.5, 1, 2, 5, and 10% (w/w) were placed into 125 mL flasks. 100 mL of inoculated BMM was then partitioned into each flask and incubated at 28 °C under static conditions. To ensure consistency in the initial microbial population, all PNCs were inoculated with the same batch of primary effluent at the same time (Madbouly et al., 2014; Volova et al., 2011). Triplicate PNC samples of each CNT loading (0–10% w/w) were removed from their reactors at each sampling time point ranging from 1 to 20 d (i.e. one full set of nanocomposites per time point). Once MWCNT/PNC samples had been removed they were not returned to the media (i.e. experiments were conducted in sacrifice mode).

Abiotic controls were setup using four replicate MWCNT/PHA nanocomposites at each CNT loading. Each abiotic control sample was sterilized with 70% ethanol for 5 min, rinsed with sterile Milli-Q water, and placed into 125 mL flasks containing 100 mL sterile BMM. Abiotic controls were incubated at 28 °C for 20 days, corresponding to the longest time point used in the biodegradation experiments.

For all mass loss measurements, the PNCs were gently removed from their flasks at the selected time point, dried in a desiccator for at least 24 h, and then weighed with a microbalance (Mettler-Toledo AT261 Delta Range, precision of ±0.015 mg). Although some biomass may have contributed to the measured mass, its mass was assumed to be much smaller than that of the CNT/PNC coupons. The percentage mass loss was calculated with respect to both the total PNC mass (Eq. (1)) and the PHA matrix mass with the presumption that EC did not biodegrade significantly over the same time course (Eq. (2)):

$$\% \text{ Total PNC Mass Loss} = \frac{\text{PNC Mass}_i - \text{PNC Mass}_t}{(\text{PNC Mass}_i)} \cdot 100 \quad (1)$$

$$\% \text{ PHA Matrix Mass Loss} = \frac{\text{PNC Mass}_i - \text{PNC Mass}_t}{(\text{PNC Mass}_i - \text{CNT Mass})} \cdot 100 \quad (2)$$

where PNC Mass_i is the total nanocomposite mass before biodegradation and PNC mass_t is the total nanocomposite mass at time *t* of primary effluent exposure. For Eq. (2), the CNT mass is defined as the mass of the CNTs and EC initially blended into the coupon. The purpose of subtracting the CNT and EC mass from the total mass of the initial PNC in Eq. (2) is to determine mass loss in terms of only the PHA matrix.

3) Dissolved Oxygen Measurements

The dissolved oxygen concentration within the inoculum was tracked, since oxygen consumption tends to increase as microorganisms metabolize a food source (OECD, 2012). To assess the oxygen availability, dissolved oxygen (DO) concentrations (mg/L) were periodically measured in experiments that contained primary effluent in contact with PHA or 10% w/w MWCNT/PHA nanocomposites. Triplicate DO measurements were collected at the onset of biodegradation, after 20 days of biodegradation, and at two time points in between (five and six days). A Hach IntelliCAL™ standard luminescent/optical DO probe (DO LDO101, 0.2–20 mg/L range, connected to a Hach multi-meter (HQ40D)) was used to make these measurements. The DO probe was sterilized with ethanol prior to use and calibrated with water-saturated air according to manufacturer specifications.

3. Results

Fig. 1a shows SEM images of PHA and MWCNT/PHA nanocomposites of varied CNT loadings (0.5, 2, and 5% w/w) before exposure to microorganisms. The surface of MWCNT/PHA nanocomposites with CNT mass loadings below 5% w/w were largely featureless with some pores visible, similar to the surface morphology of PHA (Fig. 1a and Fig. S2). In contrast, CNTs were visible at the surface of 5 and 10% w/w MWCNT/PHA nanocomposites and appear to be well dispersed in the PHA matrix (Figs. 1a and S2). This homogenous CNT distribution was supported by visual observation of a uniform CNT/PNC color for each CNT loading. Furthermore, the MWCNT/PHA nanocomposites became darker with increasing CNT loading (Fig. S1). TGA was also used to confirm the initial mass fraction of CNTs in the nanocomposite as described later. Polymer crystallinity was measured with DSC since it can influence biodegradation rates (Zhang et al., 2008). In particular, enzymatic degradation of amorphous, or less ordered domains, is more kinetically favorable than degradation of ordered, crystalline regions. This is a consequence of the fact that in crystalline regions, tightly packed polymer chains are in their most thermodynamically stable configuration and can thereby limit enzymatic access and polymer chain scission (Yildirimer et al., 2015; Tokiwa et al., 2009b). Thus, it was necessary to determine the effect (if any) of the CNT additives on PHA crystallinity. The DSC results shown in Fig. 1b and Table S1 demonstrate that the addition of MWCNTs to PHA did not change the fraction of crystalline regions in the PHA (statistics presented in Table S1). Consequently, any differences in the biodegradability of CNT/PNCs are not due to changes in polymer crystallinity.

To establish that any mass loss observed under our experimental conditions resulted exclusively from biodegradation, mass loss was determined for abiotic controls run for 20 days in the absence of primary effluent (Fig. S6). Results from these studies show that PHA did not dissolve over the course of the experiment and any mass loss observed can therefore be attributed to biodegradation by mixed culture.

Fig. 2 shows the influence of CNT loading (0, 0.5, 5 & 10% w/w) on the biodegradation kinetics of MWCNT/PHA nanocomposites as a function of incubation time in primary effluent. Fig. 2a shows the percentage of CNT/PNC mass loss, while Fig. 2b shows the percentage of PHA mass loss. The same mass loss plots are shown for 1 and 2% w/w MWCNT/

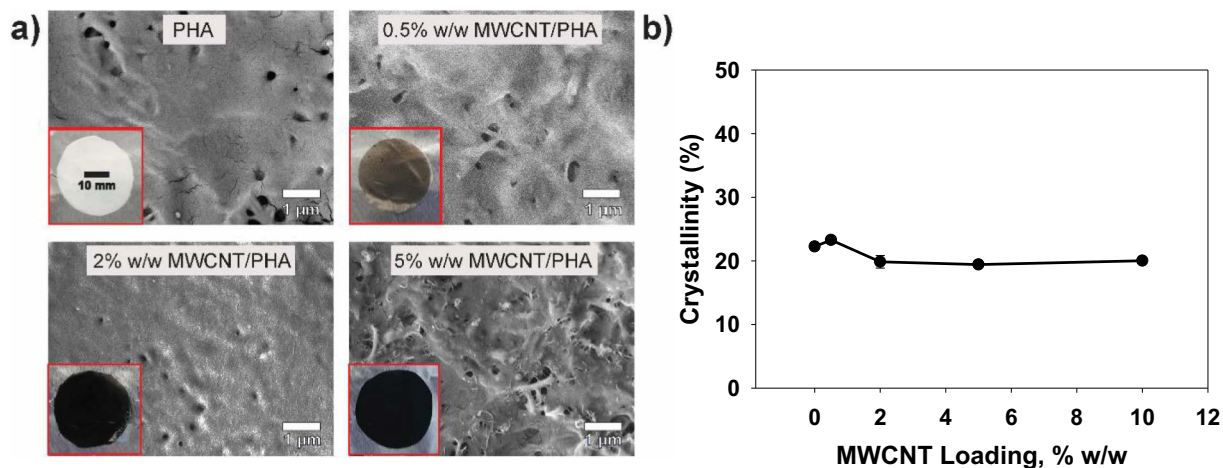


Fig. 1. a) SEM and b) DSC characterization of PHA and MWCNT/PHA nanocomposites.

PHA nanocomposites in Fig. S7. Consistent with previous studies, neat PHA readily biodegraded in the presence of an aerobic mixed culture; >90% of the PHA had biodegraded (Fig. 2a & b) after seven days, although a tenuous film remained that disintegrated upon contact (Jendrossek & Handrick, 2002; Jendrossek et al., 1993; Madbouly et al., 2014; Mas-Castellà et al., 1995; Numata et al., 2009; Ohura et al., 1999; Shah et al., 2010; Shah et al., 2008; Volova et al., 2011; Volova et al., 2010; Volova et al., 2007; Weng et al., 2011). It should be noted that although this tenuous film remained, neat PHA was plotted as 100% mass loss in Fig. 2 since this film disintegrated upon attempts to collect it and was therefore assumed to have an extremely small mass.

The data in Fig. 2a reveals that the inclusion of MWCNTs into the PHA matrix did not change the kinetics of biodegradation. Although the final %PNC mass loss did decrease systematically as the MWCNT loading increased (see inset in Fig. 2a), when the mass loss was plotted in terms of the %PHA (Fig. 2b), all of the mass loss profiles followed a single curve, with at least 90% PHA mass loss observed after 20 days, regardless of the MWCNT loading.

After 20 days of MWCNT/PHA exposure to primary effluent, the mass remaining was always approximately equal to the initial ethylcellulose content (5% w/w), some biomass (< 2% w/w), and the

initial mass of MWCNTs used to prepare the CNT/PNCs. For example, after 20 days of primary effluent exposure, the 10% w/w MWCNT/PHA nanocomposites had a residual mass equal to 16.8% of the initial PNC mass (Fig. 2a inset). Since the residual mass measured after 20 days of biodegradation was always equal to the mass of CNTs plus (5–7)% w/w, for all CNT loadings studied, the data strongly supports the idea that the vast majority of the CNT mass was retained within the initial coupon structure. The retention of MWCNTs in the nanocomposites after PHA biodegradation was further supported by TGA analysis of the 10% w/w MWCNT/PHA nanocomposites before and after primary effluent exposure (measured in air). Fig. 3a shows the weight loss of the 10% w/w MWCNT/PHA nanocomposites prior to biodegradation (measured in air). The large weight loss observed at approximately 300 °C was ascribed to the combustion of the PHA and EC. The additional 10 ± 2% (average and standard deviation of six replicates) weight loss observed between 300 and 600 °C was ascribed to the more thermally stable 10% w/w CNT mass incorporated since its profile was similar to that of the pure CNT powder in air (Fig. S4(b)) (Freiman et al., 2008; TA instruments thermal analysis, 2010). TGA was also conducted (in air) on 10% w/w MWCNT/PHA nanocomposites after 15 and 20 d of biodegradation, both corresponding to time periods where mass loss had

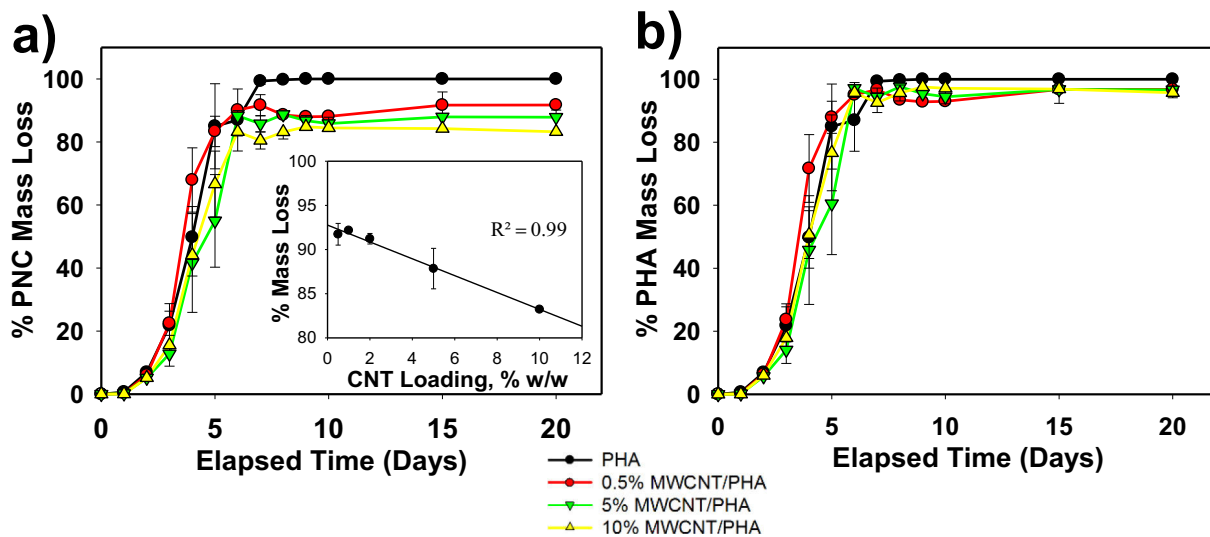


Fig. 2. Plots of a) total MWCNT/PHA nanocomposite (PNC) mass loss and b) PHA matrix mass loss (calculated as a percentage of initial PHA mass in each nanocomposite) for 0, 0.5, 5, and 10% w/w MWCNT/PHA nanocomposites. The 0% w/w MWCNT/PHA nanocomposite could not be collected at the later stages of biodegradation, so it was plotted as 100% mass loss for comparison. The inset in Fig. 2a shows that the PNC mass loss measured after 20 d decreases with the initial CNT loading, indicative of the residual CNT and ethylcellulose content in the coupon.

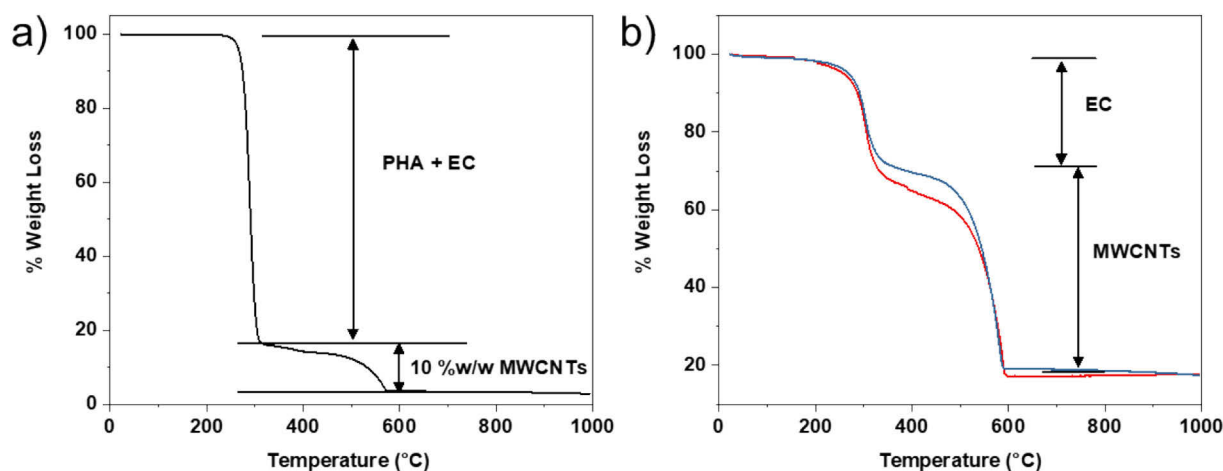


Fig. 3. TGA (in air) of 10% w/w MWCNT/PHA nanocomposites before and after primary effluent exposure. In a), the initial nanocomposite was thermally degraded, and the changes in weight associated with the thermal decomposition of PHA + EC (<math><300\text{ }^\circ\text{C}</math>) and MWCNTs (between $300\text{ }^\circ\text{C}$ and $600\text{ }^\circ\text{C}$) are indicated. In b), the residual mat left after 15 d (red) and 20 d (blue) biodegradation of MWCNT/PHA nanocomposites was analyzed by TGA. The thermal profile consisted of EC (<math><300\text{ }^\circ\text{C}</math>) and MWCNTs (between $300\text{ }^\circ\text{C}$ and $600\text{ }^\circ\text{C}$) in the same ratio as was present in the initial nanocomposites. All nanocomposites were run at a rate of $10\text{ }^\circ\text{C}/\text{min}$.

plateaued in Fig. 2. This TGA analysis was done to determine the ratio of CNTs ($300\text{--}600\text{ }^\circ\text{C}$) to polymeric material (<math><300\text{ }^\circ\text{C}</math>) and the results are shown in Fig. 3(b). Of the weight loss observed (83%), 30% was from polymeric material and 70% was from the CNTs. The residual weight that persisted above $600\text{ }^\circ\text{C}$ can be attributed to the presence of salts in the dried biofilm and residual metal/metal oxides in the CNTs (Freiman et al., 2008). Initially, the nanocomposite contained 10% w/w MWCNT and 5% w/w ethylcellulose. Therefore, if all of the PHA biodegraded, the residual biodegraded mat would be expected to be composed of 33% ethylcellulose (EC) and 67% MWCNTs (by weight). This is consistent with the 30% weight loss observed at $\approx 300\text{ }^\circ\text{C}$ (EC) and the 70% weight loss observed between 300 and $600\text{ }^\circ\text{C}$. Furthermore, when TGA was performed under an inert (argon) atmosphere, the biodegraded mat (20 d) yielded a 30:70 ratio of polymeric material to CNTs (see Fig. S5(b)), respectively, similar to the results obtained in air (Fig. 3(b)).

Under inert conditions, a comparison of the TGA data obtained from the biodegraded 10% w/w MWCNT/PHA nanocomposite (Fig. S5(b)), the MWCNT powder (Fig. S4(a)) and the initial 10% w/w MWCNTs/PHA nanocomposites (Fig. S5(a)), revealed that in all three samples the CNTs retained their thermal stability up to $800\text{ }^\circ\text{C}$. This indicated that the CNTs had not significantly lost structural integrity, become amorphous carbon, or become oxidized as a result of biodegradation (Freiman et al., 2008). Thus, the TGA data presented in Figs. 3 and S5 provides additional support for the idea that following biodegradation, the MWCNTs and EC are in the same initial ratio and the CNTs have not been transformed by the biodegradation process.

Dissolved oxygen measurements were also used to compare the biodegradation rates of PHA and 10% w/w MWCNT/PHA nanocomposites in primary effluent as shown in Fig. 4. In both cases, oxygen depletion indicated a high level of substrate (i.e. PHA matrix, acetate, and organic carbon) consumption by microorganisms, followed by a recovery period in which substrate consumption decreased and dissolved oxygen levels recovered after the PHA had been consumed (Fig. 4). With this oxygen depletion, conditions became microaerobic or possibly anaerobic at the point of maximum PHA consumption, but returned to fully aerobic conditions as the rate of mass loss/biodegradation slowed down. The large dissolved oxygen concentration drop followed by its recovery over (5, 6) days tracked with the initially high rate of PHA mass loss followed by a mass loss plateau in Fig. 4. This indicates that the majority of oxygen depletion occurred as a result of rapid PHA biodegradation. As was the case for mass loss trends, dissolved oxygen consumption trends were similar for both PHA and 10% w/w MWCNT/

PHA nanocomposites, indicating a lack of PHA biodegradation inhibition.

To determine how the MWCNT/PHA surface morphology changed as biodegradation proceeded, 5% w/w MWCNT/PHA nanocomposites were imaged with SEM before incubation, and then again after 1, 3, and 20 d of biodegradation (Figs. 5 and S8–S9). Upon incubation CNTs were initially obscured because they were embedded below the surface of the polymer and presumably some biofilm formation has occurred on the surface (Day 1). However, the accumulation of CNTs at the surface could be observed after 3 days incubation and became even more apparent after 20 days as the polymer was eroded by microorganisms as a result of biodegradation.

After 20 days of biodegradation, the surface structures of MWCNT/PHA nanocomposites with different CNT loadings (0.5, 2, 5 and 10% w/w) were imaged with SEM (Figs. 6 and S9). At all four CNT loadings, CNTs had accumulated at the surface (compare Figs. 1 and 6). However, the density of CNTs at the surface of the biodegraded 0.5 and 2% w/w

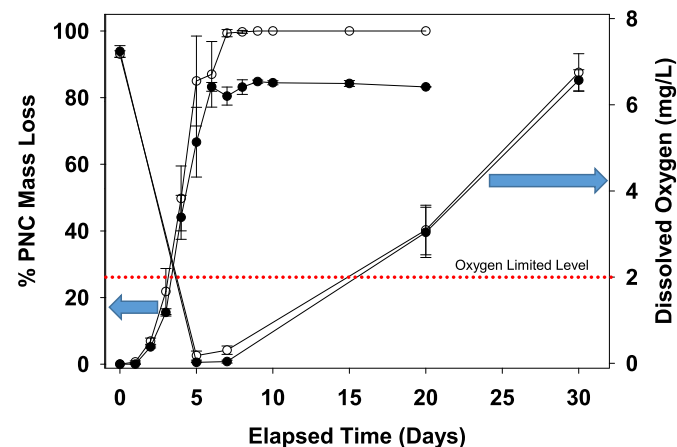


Fig. 4. Percentage of polymer nanocomposite mass loss (left arrow, plot reproduced from Fig. 2a) compared to dissolved oxygen measurements (right arrow) of PHA (unfilled circles) and 10% w/w MWCNT/PHA nanocomposites (filled circles) over the course of biodegradation in primary effluent. During the most rapid stages of PHA mass loss between 0 and 6 days, the oxygen levels become depleted (red-dotted line indicates 2 mg/L dissolved O_2 , an approximation for the start of oxygen level depletion) but the oxygen levels recover at later time points. Each DO time point is the average DO measurement of triplicate samples run over the course of 30 days.

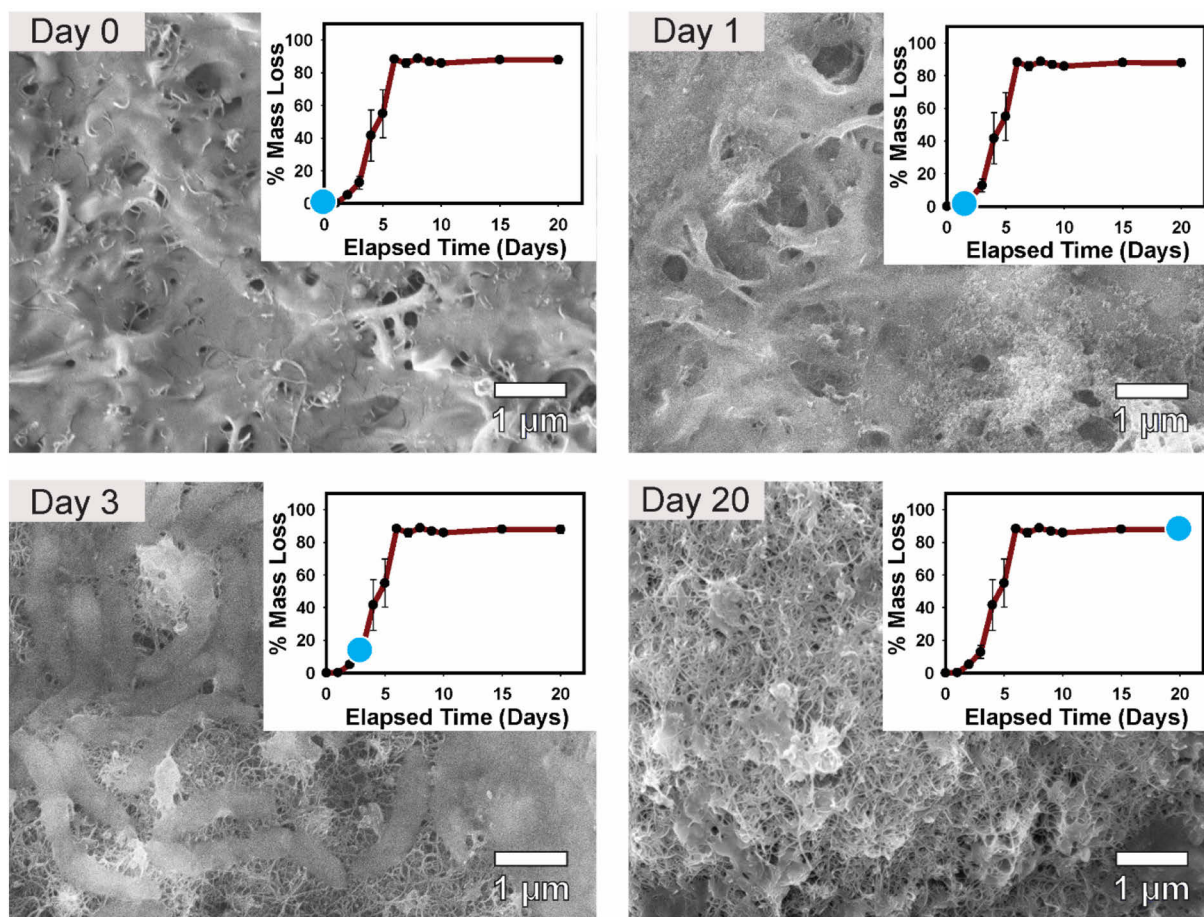


Fig. 5. SEM images of 5% w/w MWCNT/PHA nanocomposites as a function of incubation time.

MWCNT/PHA nanocomposites was significantly lower and the surface structures were more porous and diffuse as compared to the dense CNT networks observed for the 5 and 10% w/w MWCNT/PHA nanocomposites.

Although more brittle than the original CNT/PNCs, all MWCNT/PHA nanocomposites, including 0.5% w/w, maintained their two-dimensional shape and color despite the loss of >90% of the original PHA mass (Figs. 7a and S10). Since essentially all of the PHA matrix had biodegraded (Fig. 2b) and CNT surface accumulation was evident for all CNT/PNCs (Fig. 6), 20 days of mixed culture biodegradation led to the formation of CNT mats. The thicknesses of the mats formed from 5 and 10% w/w MWCNT/PHA nanocomposites were determined using cross-sectional SEM. Both 5% and 10% w/w MWCNT/PHA nanocomposites exhibited measurable decreases in thickness (Fig. S11) compared to the initial thickness of MWCNT/PHA samples, indicating that the CNTs compressed as the PHA matrix was biodegraded. An example of this decrease in thickness for a biodegraded 5% w/w MWCNT/PHA nanocomposite is shown in Fig. 7b. The average decreases in thickness of the 5 and 10% w/w MWCNT/PHA nanocomposites were 76 and 71%, respectively (Fig. 7c). It should be noted that the final thickness of the degraded CNT/PNCs may also contain a contribution from residual biomass/biofilm, meaning that the true thickness of the final CNT mat could be even less than reported.

4. Discussion

The conclusions from Fig. 2 are clear; notably that the presence of MWCNTs in the PHA matrix does not affect the rate or extent of PHA biodegradation by mixed culture. Another notable observation is that at all MWCNT loadings, CNT accumulation occurs at the surface during

polymer matrix degradation and ultimately leads to the formation of three-dimensional CNT mats (Fig. 6). There is also no indication that CNT release is occurring since the mass of the remaining CNT/PNC mat (following biodegradation) closely corresponds to the initial mass of CNTs plus the initial EC (5%) w/w at all CNT loadings. This assertion is supported by the TGA data (Figs. 3(b) and S5(b)). The absence of CNT release during biodegradation is also consistent with a previous study where we used single particle inductively coupled plasma-mass spectrometry (spICP-MS) to demonstrate the absence of Mo-containing CNT release from PCL/CNT nanocomposites during biodegradation using a single culture (Goodwin et al., 2018). Furthermore, the mass of the remaining CNT/PNC mat, which tracks with CNT loading (+EC content) also supports the claim that CNT biodegradation is not occurring in primary effluent over the timescale of these experiments. The lack of change in the thermal stability of the MWCNTs present in the biodegraded mat at high temperatures also showed that there were no significant structural or chemical changes to the CNTs during PHA biodegradation (Fig. S5(b)). Thus, if some of the MWCNTs had become oxidized or been transformed, they would not have remained stable in mass at 800 °C during TGA under an inert atmosphere (see Fig. S4(a)) (Freiman et al., 2008). Despite being more brittle than the original CNT/PNCs, all of the CNT mats retained their two-dimensional shape, even when >90% of the initial PHA matrix mass had biodegraded. Although the shape is preserved, the thickness of the CNT mats decreased significantly as compared to that of the initial PNC (see Fig. 7). This points towards a degree of CNT collapse as the surrounding polymer matrix is biodegraded, without any apparent loss of CNTs to the culture fluid. The retention of CNTs as a mat can be ascribed to the self-entanglement of CNTs within the matrix and the strong van der Waals forces between individual CNTs. The structure of the residual CNT

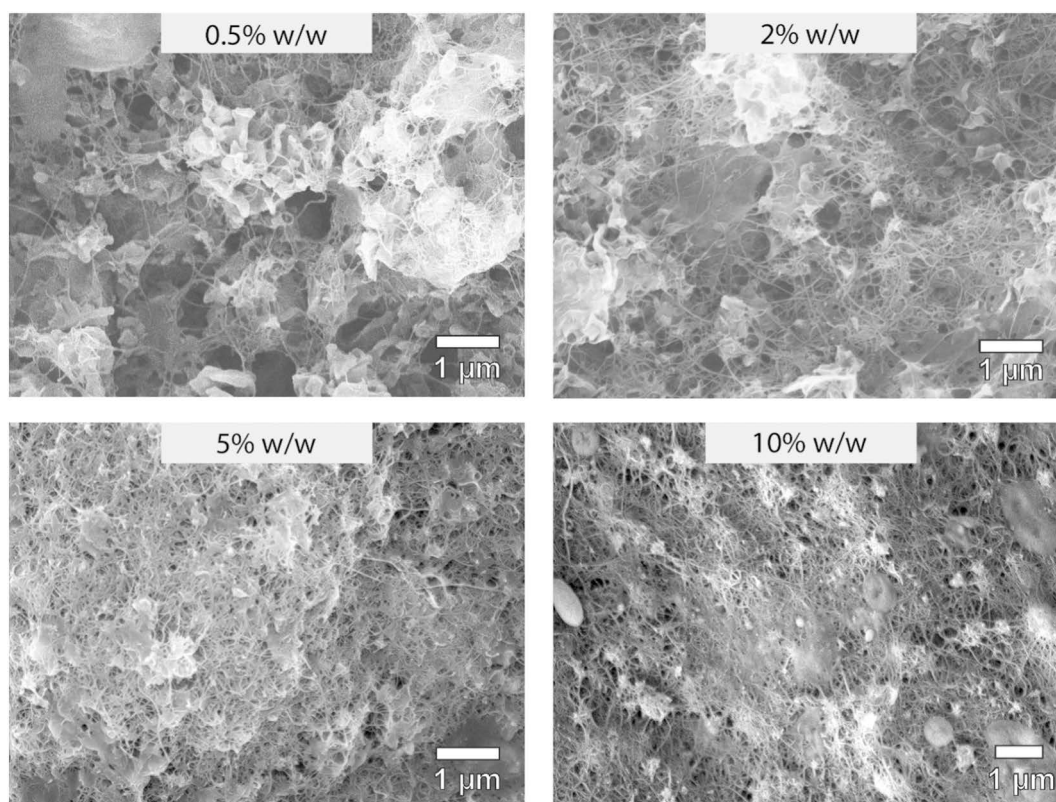


Fig. 6. SEM images showing MWCNT accumulation at the surfaces of 0.5, 2, 5, and 10% w/w MWCNT/PHA after 20 d of biodegradation.

mats was, however, influenced by the initial CNT loading, with a more porous and open structure observed with SEM for the lower MWCNT loadings (0.5 and 2% w/w MWCNT/PHA nanocomposites), presumably a reflection of the lower initial density of MWCNTs in these PNCs. Thus, the ultimate fate of the CNTs is to form a three-dimensional, interconnected, porous “mat” that will most likely remain localized at the point of biodegradation rather than being transported throughout the environment. Since the CNT mats formed from MWCNT/PHA nanocomposites at lower CNT loadings were generally more porous in structure than those with higher CNT loadings (as observed with SEM), further study on the ultimate stability of the formed CNT mats as a function of CNT loading may be warranted. Similar to other CNT/PNC degradation studies involving ultraviolet weathering, CNT release may occur from the CNT mat under mechanical stress, especially since biodegradation removes more of the polymer matrix than UV degradation processes (Schlagenhauf et al., 2015; Wohlleben et al., 2016; Nguyen et al., 2017).

The SEM images shown in Fig. 5 reveal that the nanocomposite surface morphology changes as biodegradation proceeds. During the earliest stages of CNT/PNC immersion in primary effluent (1 d) before the onset of any measurable biodegradation, a biofilm begins to form at the surface. As the polymer matrix begins to biodegrade (Days 1, 2 and 3, Figs. 5 and S8), a high density of CNTs is observed at the surface. The accumulation of the CNTs at the surface of the 5% w/w MWCNT/PHA nanocomposites after only 20% mass loss, observed by SEM (Fig. 5; Day 3), indicates that biodegradation is initiated at the PNC surface and propagates into the bulk as the incubation time increases. Indeed, CNT surface accumulation during environmental transformation processes appears to be a generalizable phenomenon, having been observed previously during weathering and thermal degradation studies of PNCs (Petersen et al., 2014; Nguyen et al., 2009; Kim et al., 2009). Despite the presence of CNTs at the surface, and more specifically the cytotoxicity they have previously been shown to impart towards a number of microorganisms (Goodwin et al., 2015; Santos et al., 2012; Lanone et al., 2013; Yang et al., 2017), continued biodegradation of the PHA matrix

by an aerobic mixed culture occurred over the full time course of the experiment (20 d).

The most striking finding of the present investigation is the lack of an inhibitory effect by MWCNTs on the biodegradation rate of PHA, across the entire range of CNT loadings studied. In contrast, we have previously observed that the presence of the same type of MWCNT had a significant inhibitory effect on the biodegradability of MWCNT/poly- ϵ -caprolactone (PCL) nanocomposites by a single culture microorganism, *P. aeruginosa*. For example, the inclusion of 5% w/w MWCNTs in PCL decreased the rate of polymer biodegradation by 82%. This marked difference in the effect of MWCNTs on polymer biodegradability is likely a reflection of the differences in the microbial population and polymer type. In the present study, PHA was exposed to the highly diverse population of microorganisms present in primary effluent. In the previous study, PCL was exposed to a single culture (*P. aeruginosa*). The inhibitory effect exerted by MWCNTs in the single culture experiment has been interpreted to be a reflection of the cytotoxic effects that CNTs (dispersed with ethylcellulose) can exert on *P. aeruginosa* (Goodwin et al., 2016). In the present study, the cytotoxic effect of CNTs could be negated by the presence of microorganisms that are not affected by CNTs or the enormous diversity of microorganisms present in a mixed culture that affords the system greater adaptability to adverse effects such as cytotoxicity or enzyme entrapment (Bhatt et al., 2008; Jendrossek & Handrick, 2002; Jendrossek et al., 1993; Madbouly et al., 2014; Mascarellà et al., 1995; Numata et al., 2009; Ohura et al., 1999; Shah et al., 2010; Shah et al., 2008; Volova et al., 2011; Volova et al., 2010; Volova et al., 2007; Weng et al., 2011; Mergaert et al., 1992). Further studies that profile the microbial communities present during biodegradation might be useful to identify the key microorganisms involved in this process. In addition to the difference in the microbial population, it is also possible that the greater ease of biodegrading PHA as compared to PCL contributes to the different effect of MWCNT incorporation; PCL biodegrades within several weeks while PHA biodegrades within a few days in primary effluent (Fig. S12). The inhibitory effect of CNTs

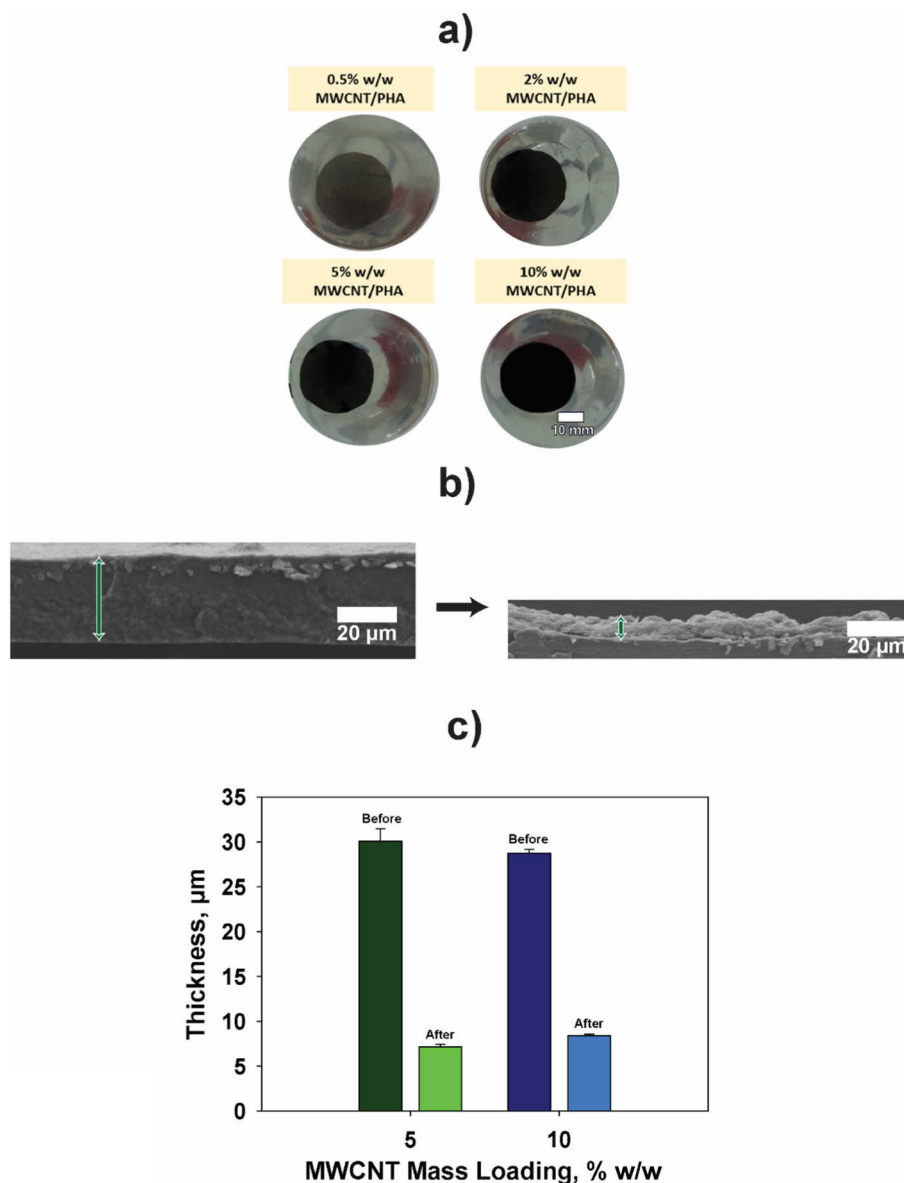


Fig. 7. a) Visually, MWCNT/PHA nanocomposites remained structurally intact after 20 days of biodegradation despite significant mass loss (>90% PHA matrix mass loss); b) a decrease in thickness of MWCNT/PHA nanocomposites following 20 d of biodegradation was observed using cross-sectional SEM (5% w/w shown as an example) and thicknesses were measured in six similarly spaced locations across the sample; c) the average thickness of duplicate 5% w/w and a single 10% w/w MWCNT/PHA nanocomposite before and after biodegradation which were each measured in triplicate areas (6 measurements per area) using ImageJ software.

are likely to be less pronounced when the substrate (polymer) is more easily metabolized with a lower overall activation energy for biodegradation. If a rapidly degradable polymer matrix is used, microorganisms in a mixed culture will most likely be able to adapt or make use of bacteria strains that are less affected by the CNTs to consume the polymer despite the stress or cytotoxicity caused by the presence of CNTs. In contrast to the lack of inhibitory effect reported here, another study observed some inhibitory effects of graphene oxide (GO) nanofiller, on polysulfone (PSU) biodegradation in primary effluent. This effect was ascribed to the cytotoxicity of GO (Peña-Bahamonde et al., 2018). The inhibitory effects observed were most likely a consequence of slower PSU biodegradation as compared to the rapid rate of PHA biodegradation observed in this study. Further study on the effect of CNT fillers on biodegradation of polymers with different rates of biodegradability in both single and mixed culture will provide insight on the mechanisms and extents to which microorganisms adapt to the presence of nanomaterials in consumer polymer nanocomposites. Collectively, our results suggest that the inhibitive effects of CNTs on biodegradation

previously observed for model microorganisms will most likely matter less in the environment where there are diverse microbial communities such as in wastewater, surface water, and soil.

5. Conclusions

This study has shown that the incorporation of MWCNTs does not affect the rate or extent of PHA matrix biodegradation in MWCNT/PHA nanocomposites exposed to primary effluent. Even at MWCNT loadings as high as 10% w/w, there is no effect on the rate or removal of the PHA content in the nanocomposite despite the known cytotoxic effects of CNTs towards a number of microorganisms (Goodwin et al., 2015; Santos et al., 2012; Lanone et al., 2013; Yang et al., 2017). Instead, almost complete PHA matrix biodegradation occurs, leaving behind a compressed CNT mat with a thickness that decreased by over 70% for MWCNT/PHA nanocomposites with >5% w/w MWCNTs. Experimental evidence indicates that at the conclusion of PHA biodegradation, this residual CNT mat contained the same CNT mass initially present in the

nanocomposite, which indicates that no measurable CNT release occurred during biodegradation. As a consequence, CNTs initially present in biodegradable polymer matrices will most likely remain localized at the point of biodegradation as an interlinked mat rather than being transported throughout the environment. As evidenced by TGA data, CNTs do not significantly transform during polymer biodegradation and are likely to remain persistent in the environment. This may affect organisms that make contact with the CNT mat in the environment, but the large size of the CNT mat formed is likely to limit uptake of CNTs by smaller organisms that leads to bioaccumulation and/or biomagnification. Residual CNT mats with their high surface areas may also serve as “sponges” for the adsorption of water borne contaminants such as hydrophobic organic chemicals. Further study on the mechanical stability of the CNT mats formed as well as different biodegradable polymer types that could be used for biological recycling of CNT/PNCs would be useful.

Acknowledgements

The authors would also like to thank the National Science Foundation (CBET #1236493) and the JHU INBT Pilot Project. David Goodwin acknowledges the JHU Department of Chemistry for the Owens Graduate Fellowship which helped to support this work. Duc Phan thanks the Vietnam Education Foundation for funding. The authors would also like to thank Marshall Phillips at the Back River Wastewater Treatment Plant in Baltimore, MD for supplying the primary effluent to support this project.

Appendix A. Supplementary data

Additional information is provided on CNT/PNC preparation, images of prepared PHA and MWCNT/PHA nanocomposites (Fig. S1); differential scanning calorimetry results (Table S1); EDS methods and results for residual solvent and MWCNT metal content (Tables S2 and S3), information on BMM composition; SEM analysis and replicate SEM images of PHA and MWCNT/PHA nanocomposites before biodegradation (Fig. S2); TGA analysis of PHA (containing EC) under inert conditions (Fig. S3); TGA analysis of the MWCNT powder used in this study under air and inert conditions (Fig. S4); TGA analysis of 10% w/w MWCNT/PHA nanocomposites before and after 20 d primary effluent exposure under inert conditions (Fig. S5); abiotic control PNC mass loss plots (Fig. S6); PNC mass loss and PHA matrix mass loss plots of 1 and 2% w/w MWCNT/PHA nanocomposites (Fig. S7); replicate SEM images of 5% w/w MWCNT/PHA nanocomposites after 1, 2, and 3 d of biodegradation (Fig. S8); replicate SEM images of 0.5, 2, 5 and 10% w/w MWCNT/PHA nanocomposites (two separately prepared samples for 5% w/w to show MWCNT/PHA sample-to-sample consistency) after 20 d of biodegradation (Fig. S9); images of PHA and 1% w/w MWCNT/PHA nanocomposites that remained structurally intact after 20 d of biodegradation despite significant mass loss (>90% PHA matrix mass loss) (Fig. S10); cross-sectional SEM images of 5 and 10% (w/w) MWCNT/PHA nanocomposites before and after 20 d biodegradation to measure thickness decreases (Fig. S11); and a comparison of PCL (4% w/w EC) and PHA (5% w/w EC) biodegradation in primary effluent on the same mass loss plot (Fig. S12). Supplementary data to this article can be found online at doi:<https://doi.org/10.1016/j.scitotenv.2018.05.137>.

References

- Aider, M., 2010. Chitosan application for active bio-based films production and potential in the food industry: review. *LWT Food Sci. Technol.* 43, 837–842.
- Armentano, I., Dottori, M., Fortunati, E., Mattioli, S., Kenny, J.M., 2010. Biodegradable polymer matrix nanocomposites for tissue engineering: a review. *Polym. Degrad. Stab.* 95 (11), 2126–2146.
- ASTM, A.S.f.T.a.M.-D., 1996. 6003–96: Standard Test Method for Determining Weight Loss from Plastic Materials Exposed to Simulated Municipal Solid-Waste (MSW) Aerobic Compost Environment. Annual Book of ASTM Standards: Philadelphia.
- Barham, P.J., Keller, A., Otun, E.L., Holmes, P.A., 1984. Crystallization and morphology of a bacterial thermoplastic: poly-3-hydroxybutyrate. *J. Mater. Sci.* 19 (9), 2781–2794.
- Bhatt, R., Shah, D., Patel, K., Trivedi, U., 2008. PHA–rubber blends: synthesis, characterization and biodegradation. *Bioresour. Technol.* 99 (11), 4615–4620.
- Calmon, A., Dusserre-Bresson, L., Bellon-Maurel, V., Feuilloley, P., Silvestre, F., 2000. An automated test for measuring polymer biodegradation. *Chemosphere* 41 (5), 645–651.
- Chen, M., Qin, X., Zeng, G., 2017. Biodegradation of carbon nanotubes, graphene, and their derivatives. *Trends Biotechnol.* 35 (9), 836–846.
- Coleman, J.N., Khan, U., Blau, W.J., Gun'ko, Y.K., 2006. Small but strong: a review of the mechanical properties of carbon nanotube–polymer composites. *Carbon* 44 (9), 1624–1652.
- De, V.M.F.L., Tawfik, S.H., Baughman, R.H., Hart, A.J., 2013. Carbon nanotubes: present and future commercial applications. *Science* 339 (6119), 535–539.
- Deshmukh, S., Mhadeshwar, N., 2011. Biodegradable polymers. *Pop. Plast. Packag.* 56 (9), 48–52.
- Du, J.-H., Bai, J., Cheng, H.M., 2007. The present status and key problems of carbon nanotube based polymer composites. *Express Polym Lett* 5, 253–272.
- EPA, 2001. 5210B Biochemical Oxygen Demand (BOD) Standard Method. In United States of America.
- Fama, L.M., Pettarin, V., Goyanes, S.N., Bernal, C.R., 2011. Starch/multi-walled carbon nanotubes composites with improved mechanical properties. *Carbohydr. Polym.* 83 (3), 1226–1231.
- Fan, J., Grande, C.D., Rodrigues, D.F., 2017. Biodegradation of graphene oxide–polymer nanocomposite films in wastewater. *Environ. Sci. Nano* 4 (9), 1808–1816.
- Freiman, S., Hooker, S., Migler, K., Arepalli, S., 2008. Measurement Issues in Single Wall Carbon Nanotubes. National Institute of Standards and Technology, Special Publication, Washington, USA.
- Freixa, A., Acuña, V., Sanchís, J., Farré, M., Barceló, D., Sabater, S., 2018. Ecotoxicological effects of carbon based nanomaterials in aquatic organisms. *Sci. Total Environ.* 619, 328–337.
- Gilmore, D.F., Antoun, S., Lenz, R.W., Fuller, R.C., 1993. Degradation of poly (β -hydroxyalkanoates) and polyolefin blends in a municipal wastewater treatment facility. *J. Environ. Polym. Degrad.* 1 (4), 269–274.
- Ging, J., Tejerina-Anton, R., Ramakrishnan, G., Nielsen, M., Murphy, K., Gorham, J.M., Nguyen, T., Orlov, A., 2014. Development of a conceptual framework for evaluation of nanomaterials release from nanocomposites: environmental and toxicological implications. *Sci. Total Environ.* 473, 9–19.
- Goodwin Jr, D.G., Boyer, I., Devahif, T., Gao, C., Frank, B.P., Lu, X., Kuwama, L., Gordon, T.B., Wang, J., Ranville, J.F., 2018. Biodegradation of carbon nanotube/polymer nanocomposites using a monoculture. *Environ. Sci. Technol.* 52 (1), 40–51.
- Goodwin, D.G., Marsh, K.M., Sosa, I.B., Payne, J.B., Gorham, J.M., Bouwer, E.J., Fairbrother, D.H., 2015. Interactions of microorganisms with polymer nanocomposite surfaces containing oxidized carbon nanotubes. *Environ. Sci. Technol.* 49 (9), 5484–5492.
- Goodwin, D.G., Xia, Z., Gordon, T.B., Gao, C., Bouwer, E.J., Fairbrother, D.H., 2016. Biofilm development on carbon nanotube/polymer nanocomposites. *Environ. Sci. Nano* 3 (3), 545–558.
- Gottschalk, F., Nowack, B., 2011. The release of engineered nanomaterials to the environment. *J. Environ. Monit.* 13 (5), 1145–1155.
- Gupta, A., Woods, M.D., Illingworth, K.D., Niemeier, R., Schafer, I., Cady, C., Filip, P., El-Amin, S.F., 2013. Single walled carbon nanotube composites for bone tissue engineering. *J. Orthop. Res.* 31 (9), 1374–1381.
- Harrison, B.S., Atala, A., 2007. Carbon nanotube applications for tissue engineering. *Biomaterials* 28 (2), 344–353.
- Hossain, F., Perales-Perez, O.J., Hwang, S., Roman, F., 2014. Antimicrobial nanomaterials as water disinfectant: applications, limitations and future perspectives. *Sci. Total Environ.* 466, 1047–1059.
- Huh, M., Jung, M.H., Park, Y.S., Kim, B.-J., Kang, M.S., Holden, P.J., Yun, S.I., 2014. Effect of carbon nanotube functionalization on the structure and properties of poly(3-hydroxybutyrate)/MWCNTs biocomposites. *Macromol. Res.* 22 (7), 765–772.
- Itävaara, M., Vikman, M., 1996. An overview of methods for biodegradability testing of biopolymers and packaging materials. *J. Environ. Polym. Degrad.* 4 (1), 29–36.
- Jendrossek, D., Handrick, R., 2002. Microbial degradation of polyhydroxyalkanoates. *Annu. Rev. Microbiol.* 56 (1), 403–432.
- Jendrossek, D., Knoke, I., Habibi, R.B., Steinbüchel, A., Schlegel, H.G., 1993. Degradation of poly(3-hydroxybutyrate), PHB, by bacteria and purification of a novel PHB depolymerase from *Comamonas* sp. *J. Environ. Polym. Degrad.* 1 (1), 53–63.
- Khatiwala, V.K., Shekhar, N., Aggarwal, S., Mandal, U.K., 2008. Biodegradation of poly(ϵ -caprolactone) (PCL) film by *Alcaligenes faecalis*. *J. Polym. Environ.* 16 (1), 61–67.
- Kim, J.Y., 2009. Carbon nanotube-reinforced thermotropic liquid crystal polymer nanocomposites. *Dent. Mater.* 2 (4), 1955–1974.
- Kim, J.Y., Park, H.S., Kim, S.H., 2009. Thermal decomposition behavior of carbon nanotube-reinforced poly (ethylene 2, 6-naphthalate) nanocomposites. *J. Appl. Polym. Sci.* 113 (3), 2008–2017.
- Krzan, A., Hemjinda, S., Miertus, S., Corti, A., Chiellini, E., 2006. Standardization and certification in the area of environmentally degradable plastics. *Polym. Degrad. Stab.* 91 (12), 2819–2833.
- Kumar, A.P., Depan, D., Tomer, N.S., Singh, R.P., 2009. Nanoscale particles for polymer degradation and stabilization—trends and future perspectives. *Prog. Polym. Sci.* 34 (6), 479–515.
- Lanone, S., Andujar, P., Kermanizadeh, A., Boczkowski, J., 2013. Determinants of carbon nanotube toxicity. *Adv. Drug Deliv. Rev.* 65 (15), 2063–2069.
- Lee, S.Y., Choi, J.-I., Wong, H.H., 1999. Recent advances in polyhydroxyalkanoate production by bacterial fermentation: mini-review. *Int. J. Biol. Macromol.* 25 (1–3), 31–36.
- Leja, K., Lewandowicz, G., 2010. Polymer biodegradation and biodegradable polymers—a review. *Pol. J. Environ. Stud.* 19 (2), 255–266.

- Liao, H.-T., Wu, C.-S., 2013. Poly (3-hydroxybutyrate)/multi-walled carbon nanotubes nanocomposites: preparation and characterizations. *Des. Monomers Polym.* 16 (2), 99–107.
- Luckachan, G.E., Pillai, C.K.S., 2011. Biodegradable polymers—a review on recent trends and emerging perspectives. *J. Polym. Environ.* 19 (3), 637–676.
- Madbouly, S.A., Schrader, J.A., Srinivasan, G., Liu, K., McCabe, K.G., Grewell, D., Graves, W.R., Kessler, M.R., 2014. Biodegradation behavior of bacterial-based polyhydroxyalkanoate (PHA) and DDGS composites. *Green Chem.* 16 (4), 1911–1920.
- Maiti, P., Prakash Yadav, J.P., 2008. Biodegradable nanocomposites of poly (hydroxybutyrate-co-hydroxyvalerate): the effect of nanoparticles. *J. Nanosci. Nanotechnol.* 8 (4), 1858–1866.
- Mas-Castellà, J., Urmeneta, J., Lafuente, R., Navarrete, A., Guerrero, R., 1995. Biodegradation of poly-β-hydroxyalkanoates in anaerobic sediments. *Int. Biodeterior. Biodegrad.* 35 (1–3), 155–174.
- Massardier-Nageotte, V., Pestre, C., Cruard-Pradet, T., Bayard, R., 2006. Aerobic and anaerobic biodegradability of polymer films and physico-chemical characterization. *Polym. Degrad. Stab.* 91 (3), 620–627.
- Mattioli-Belmonte, M., Vozzi, G., Whulanza, Y., Seggiani, M., Fantauzzi, V., Orsini, G., Ahluwalia, A., 2012. Tuning polycaprolactone-carbon nanotube composites for bone tissue engineering scaffolds. *Mater. Sci. Eng. C* 32 (2), 152–159.
- Mergaert, J., Anderson, C., Wouters, A., Swings, J., Kersters, K., 1992. Biodegradation of polyhydroxyalkanoates. *FEMS Microbiol. Lett.* 103 (2–4), 317–321.
- Miretzky, P., Cirelli, A.F., 2011. Fluoride removal from water by chitosan derivatives and composites: a review. *J. Fluor. Chem.* 132, 231–240.
- Misra, S.K., Valappil, S.P., Roy, I., Boccacini, A.R., 2006. Polyhydroxyalkanoate (PHA)/inorganic phase composites for tissue engineering applications. *Biomacromolecules* 7 (8), 2249–2258.
- Mittal, V., 2011. *Nanocomposites with Biodegradable Polymers: Synthesis, Properties, and Future Perspectives*. Oxford University Press.
- Mohee, R., Unmar, G.D., Mudhoo, A., Khadoo, P., 2008. Biodegradability of biodegradable/degradable plastic materials under aerobic and anaerobic conditions. *Waste Manage. (Amsterdam, Neth.)* 28 (9), 1624–1629.
- Moniruzzaman, M., Winey, K.L., 2006. Polymer nanocomposites containing carbon nanotubes. *Macromolecules* 39 (16), 5194–5205.
- Nguyen, T., Pellegrin, B., Mermet, L., Shapiro, A., Gu, X., Chin, J., 2009. Network aggregation of CNTs at the surface of epoxy/MWCNT composite exposed to UV radiation. *Nanotechnology* 90–93.
- Nguyen, T., Petersen, E.J., Pellegrin, B., Gorham, J.M., Lam, T., Zhao, M., Sung, L., 2017. Impact of UV irradiation on multiwall carbon nanotubes in nanocomposites: formation of entangled surface layer and mechanisms of release resistance. *Carbon* 116, 191–200.
- Numata, K., Abe, H., Iwata, T., 2009. Biodegradability of poly (hydroxyalkanoate) materials. *Materials* 2 (3), 1104–1126.
- OECD, 2012. *Detailed Review Paper on Biodegradability Testing*. OECD Publishing.
- Ohura, T., Aoyagi, Y., Takagi, K.-i., Yoshida, Y., Kasuya, K.-i., Doi, Y., 1999. Biodegradation of poly(3-hydroxyalkanoic acids) fibers and isolation of poly(3-hydroxybutyric acid)-degrading microorganisms under aquatic environments. *Polym. Degrad. Stab.* 63 (1), 23–29.
- Pagga, U., Schäfer, A., Müller, R.-J., Pantke, M., 2001. Determination of the aerobic biodegradability of polymeric material in aquatic batch tests. *Chemosphere* 42 (3), 319–331.
- Pan, L., Pei, X., He, R., Wan, Q., Wang, J., 2012. Multiwall carbon nanotubes/polycaprolactone composites for bone tissue engineering application. *Colloids Surf., B* 93, 226–234.
- Parks, A.N., Chandler, G.T., Ho, K.T., Burgess, R.M., Ferguson, P.L., 2015. Environmental biodegradability of [14C] single-walled carbon nanotubes by *Trametes versicolor* and natural microbial cultures found in New Bedford Harbor sediment and aerated wastewater treatment plant sludge. *Environ. Toxicol. Chem.* 34 (2), 247–251.
- Pelegrini, K., Donazzolo, I., Brambilla, V., Coulon Grisa, A.M., Piazza, D., Zattera, A.J., Brandalise, R.N., 2016. Degradation of PLA and PLA in composites with triacetin and buriti fiber after 600 days in a simulated marine environment. *J. Appl. Polym. Sci.* 133 (15) (n/a–n/a).
- Peña-Bahamonde, J., San-Miguel, V., Cabanelas, J., Rodrigues, D., 2018. Biological degradation and biostability of nanocomposites based on polysulfone with different concentrations of reduced graphene oxide. *Macromol. Mater. Eng.* 303 (2), 1700359.
- Petersen, E.J., Zhang, L.W., Mattison, N.T., O'Carroll, D.M., Whelton, A.J., Uddin, N., Nguyen, T., Huang, Q.G., Henry, T.B., Holbrook, R.D., Chen, K.L., 2011. Potential release pathways, environmental fate, and ecological risks of carbon nanotubes. *Environ. Sci. Technol.* 45 (23), 9837–9856.
- Petersen, E.J., Lam, T., Gorham, J.M., Scott, K.C., Long, C.J., Stanley, D., Sharma, R., Alexander Liddle, J., Pellegrin, B., Nguyen, T., 2014. Methods to assess the impact of UV irradiation on the surface chemistry and structure of multiwall carbon nanotube epoxy nanocomposites. *Carbon* 69, 194–205.
- Posen, I.D., Jaramillo, P., Griffin, W.M., 2016. Uncertainty in the life cycle greenhouse gas emissions from U.S. production of three biobased polymer families. *Environ. Sci. Technol.* 50 (6), 2846–2858.
- Premraj, R., Doble, M., 2005. Biodegradation of polymers. *Indian J. Biotechnol.* 4, 186–193.
- Qiu, Z., Wang, H., Xu, C., 2011. Crystallization, mechanical properties, and controlled enzymatic degradation of biodegradable poly(ε-caprolactone)/multi-walled carbon nanotubes nanocomposites. *Nanosci. Nanotechnol.* 11, 7884–7893.
- Sahoo, N.G., Rana, S., Cho, J.W., Li, L., Chan, S.H., 2010. Polymer nanocomposites based on functionalized carbon nanotubes. *Prog. Polym. Sci.* 35 (7), 837–867.
- Santos, C.M., Milagros Cui, K., Ahmed, F., Tria, M.C.R., Vergara, R.A.M.V., de Leon, A.C., Advincula, R.C., Rodrigues, D.F., 2012. Bactericidal and anticorrosion properties in PVK/MWNT nanocomposite coatings on stainless steel. *Macromol. Mater. Eng.* 297 (8), 807–813.
- Sarkar, B., Mandal, S., Tsang, Y.F., Kumar, P., Kim, K.-H., Ok, Y.S., 2018. Designer carbon nanotubes for contaminant removal in water and wastewater: a critical review. *Sci. Total Environ.* 612, 561–581.
- Schlagenhauf, L., Kianfar, B., Buerki-Thurnherr, T., Kuo, Y.-Y., Wichser, A., Nuesch, F., Wick, P., Wang, J., 2015. Weathering of a carbon nanotube/epoxy nanocomposite under UV light and in water bath: impact on abraded particles. *Nano* 7 (44), 18524–18536.
- Shah, A.A., Hasan, F., Hameed, A., Ahmed, S., 2008. Biological degradation of plastics: a comprehensive review. *Biotechnol. Adv.* 26 (3), 246–265.
- Shah, A.A., Hasan, F., Hameed, A., 2010. Degradation of poly(3-hydroxybutyrate-co-3-hydroxyvalerate) by a newly isolated *Actinomadura* sp. AF-555, from soil. *Int. Biodeterior. Biodegrad.* 64 (4), 281–285.
- Singh, N.K., Purkayastha, B.P.D., Roy, J.K., Banik, R.M., Gonugunta, P., Misra, M., Maiti, P., 2011. Tuned biodegradation using poly (hydroxybutyrate-co-valerate) nanobiohybrids: emerging biomaterials for tissue engineering and drug delivery. *J. Mater. Chem.* 21 (40), 15919–15927.
- Strotmann, U., Reuschenbach, P., Schwarz, H., Pagga, U., 2004. Development and evaluation of an online CO₂ evolution test and a multicomponent biodegradation test system. *Appl. Environ. Microbiol.* 70 (8), 4621–4628.
- Stuart, B.H., 2008. *Polymer Analysis*. Vol. 30. John Wiley & Sons.
- Sudesh, K., 2012. *Polyhydroxyalkanoates from Palm Oil: Biodegradable Plastics*. Springer Science & Business Media.
- TA instruments thermal analysis. In SDT Q600 Specifications. TA Instruments.
- Tokiwa, Y., Calabria, B.P., Ugwu, C.U., Alba, S., 2009a. Biodegradability of plastics. *Int. J. Mol. Sci.* 10 (9), 3722–3742.
- Tokiwa, Y., Calabria, B.P., Ugwu, C.U., Aiba, S., 2009b. Biodegradability of plastics. *Int. J. Mol. Sci.* 10 (9), 3722–3742.
- Tsuji, H., Kawashima, Y., Takikawa, H., Tanaka, S., 2007. Poly(l-lactide)/nano-structured carbon composites: conductivity, thermal properties, crystallization, and biodegradation. *Polymer* 48 (14), 4213–4225.
- Velasco-Santos, C., Martínez-Hernández, A.L., Fisher, F.T., Ruoff, R., Castañó, V.M., 2003. Improvement of thermal and mechanical properties of carbon nanotube composites through chemical functionalization. *Chem. Mater.* 15 (23), 4470–4475.
- Volova, T.I.a.G.e., 2004. *Polyhydroxyalkanoates—Plastic Materials of the 21st Century: Production, Properties, Applications*. Nova Publishers.
- Volova, T.G., Gladyshev, M.I., Trusova, M.Y., Zhila, N.O., 2007. Degradation of polyhydroxyalkanoates in eutrophic reservoir. *Polym. Degrad. Stab.* 92 (4), 580–586.
- Volova, T.G., Boyandin, A.N., Vasiliev, A.D., Karpov, V.A., Prudnikova, S.V., Mishukova, O.V., Boyarskikh, U.A., Filipenko, M.L., Rudnev, V.P., Bá Xuân, B., Việt Dũng, V., Gitelson, I.I., 2010. Biodegradation of polyhydroxyalkanoates (PHAs) in tropical coastal waters and identification of PHA-degrading bacteria. *Polym. Degrad. Stab.* 95 (12), 2350–2359.
- Volova, T.G., Boyandin, A.N., Vasil'ev, A.D., Karpov, V.A., Kozhevnikov, I.V., Prudnikova, S.V., Rudnev, V.P., Xuân, B.B., Dũng, V.V., Gitel'zon, I.I., 2011. Biodegradation of polyhydroxyalkanoates (PHAs) in the South China Sea and identification of PHA-degrading bacteria. *Microbiology* 80 (2), 252–260.
- Wan Ngh, W.S., Teong, L.C., Hanafiah, M.A.K.M., 2011. Adsorption of dyes and heavy metal ions by chitosan composites: a review. *Carbohydr. Polym.* 83, 1446–1456.
- Wang, S.-F., Shen, L., Zhang, W.-D., Tong, Y.-J., 2005. Preparation and mechanical properties of chitosan/carbon nanotubes composites. *Biomacromolecules* 6, 3067–3072.
- Weng, Y.-X., Wang, X.-L., Wang, Y.-Z., 2011. Biodegradation behavior of PHAs with different chemical structures under controlled composting conditions. *Polym. Test.* 30 (4), 372–380.
- Wohlleben, W., Meyer, J., Müller, P., Vilsmeier, K., Stahlmecke, B., Kuhlbusch, T.A., 2016. Release from nanomaterials during their use phase: combined mechanical and chemical stresses applied to simple and multi-filler nanocomposites mimicking wear of nano-reinforced tires. *Environ. Sci.: Nano* 3 (5), 1036–1051.
- Wu, C.-S., 2005. A comparison of the structure, thermal properties, and biodegradability of polycaprolactone/chitosan and acrylic acid grafted polycaprolactone/chitosan. *Polymer* 46 (1), 147–155.
- Wu, C.-S., Liao, H.-T., 2007. Study on the preparation and characterization of biodegradable polylactide/multi-walled carbon nanotubes nanocomposites. *Polymer* 48 (15), 4449–4458.
- Wu, D., Wu, L., Zhou, W., Zhang, M.Y., Yang, T., 2010. Crystallization and biodegradation of polylactide carbon nanotube composites. *Polym. Eng. Sci.* 50 (9), 1721–1733.
- Yang, F., Jiang, Q., Zhu, M., Zhao, L., Zhang, Y., 2017. Effects of biochars and MWNTs on biodegradation behavior of atrazine by *Acinetobacter lwoffii* DNS32. *Sci. Total Environ.* 577, 54–60.
- Yildirim, L., Bunaz, A., Gaisford, S., Malins, E.L., Remzi Becer, C., Moiem, N., Reynolds, G.M., Seifalian, A.M., 2015. Controllable degradation kinetics of POSS nanoparticle-integrated poly(ε-caprolactone urea)urethane elastomers for tissue engineering applications. *Sci. Rep.* 5, 15040.
- Yun, S.I., Gadd, G.E., Latella, B.A., Lo, V., Russell, R.A., Holden, P.J., 2008. Mechanical properties of biodegradable polyhydroxyalkanoates/single wall carbon nanotube nanocomposite films. *Polym. Bull.* 61 (2), 267–275.
- Zaman, I., Manshoor, B., Khalid, A., Araby, S., 2014. From clay to graphene for polymer nanocomposites—a survey. *J. Polym. Res.* 21 (5), 1–11.
- Zeng, H.L., Gao, C., Yan, D.Y., 2006. Poly(ε-caprolactone)-functionalized carbon nanotubes and their biodegradation properties. *Adv. Funct. Mater.* 16 (6), 812–818.
- Zhang, S., Li, L., Kumar, A., 2008. *Materials Characterization Techniques*. CRC Press.
- Zhang, L., Petersen, E.J., Habteselassie, M.Y., Mao, L., Huang, Q., 2013. Degradation of multiwall carbon nanotubes by bacteria. *Environ. Pollut. (Oxford, U. K.)* 181, 335–339.